PROCEEDINGS OF SCIENCE

ONLINE ICRC 2021
THE ASTROPARTICLE PHYSICS CONFERENCE
Berlin | Germany
37th International Cosmic Ray Conference
12–23 July 2021

Modelling uncertainties in GeV – TeV flux predictions of Galactic globular clusters

Christo Venter,[a,*] **Hambeleleni Davids,**[a,b] **Andreas Kopp**[a] **and Michael Backes**[c,a]

[a] *Centre for Space Research, North-West University, Potchefstroom Campus, Private Bag X6001, Potchefstroom 2520, South Africa*

[b] *Department of Science Foundation, School of Science, University of Namibia, Private Bag 13301, Windhoek 10005, Namibia*

[c] *University of Namibia, Department of Physics, Chemistry & Material Science, Windhoek Campus, Private Bag 13301, Windhoek, Namibia*

E-mail: christo.venter@nwu.ac.za, hndiyavala@unam.na, ak@tp4.ruhr-uni-bochum.de, mbackes@unam.na

Globular clusters are multi-band emitters, with their gamma-ray emission having been variously attributed to dark matter annihilation, a resident gamma-ray burst, or collective emission from a white-dwarf or millisecond-pulsar population hosted by the cluster. Terzan 5 has plausibly been detected in the gamma-ray band by H.E.S.S., which also produced constraining stacking upper limits on the integral gamma-ray fluxes of a population of other Galactic globular clusters. Using a leptonic model that invokes host millisecond pulsars in globular clusters as sources of relativistic particles, we perform three case studies. First, we demonstrate that uncertainty in model parameters leads to a large spread in the predicted gamma-ray flux for a population of clusters, yet there are regions in parameter space for which the stringent H.E.S.S. stacking upper limits are satisfied. Two additional case studies on M15 (for which MAGIC recently derived stringent differential flux upper limits) and ω Cen (from which five pulsars have recently been detected at radio frequencies) indicate that it is vital to increase measurement accuracy on key model parameters to improve precision in predictions of cluster fluxes. This has important implications for the observational strategy of the CTA.

37th International Cosmic Ray Conference (ICRC 2021)
July 12th – 23rd, 2021
Online – Berlin, Germany

*Presenter

PoS(ICRC2021)927

1. Introduction

There are about 160 Galactic globular clusters (GCs) associated with our Milky Way [1]. These sources emit photons across the electromagnetic spectrum. About 20 of these GCs have been detected in the GeV band by the *Fermi* Large Area Telescope (LAT) [2–4]. The High Energy Stereoscopic System (H.E.S.S.) has plausibly detected a single GC in our Galaxy, i.e., Terzan 5 [5], in the very-high-energy (VHE; $E > 100$ GeV) band and also published VHE upper limits from 15 other GCs [6]. A more sensitive stacking analysis involving a live-time-weighted flux of these 15 GCs resulted only in upper limits. Other Cherenkov telescopes also produced upper limits (e.g., [7]). The Major Atmospheric Gamma Imaging Cherenkov Telescopes (MAGIC) provided a deep upper limit on M15 of $F(E > 300\,\mathrm{GeV})$, i.e., $< 0.26\%$ of the Crab Nebula flux. Stringent differential flux upper limits were also obtained [8]. Earlier, H.E.S.S. published an upper limit on the integral flux of 47 Tucanae of $F(E > 800\,\mathrm{GeV}) < 6.7 \times 10^{-13}\,\mathrm{cm}^{-2}\mathrm{s}^{-1}$ [9].

Several leptonic and hadronic models predict the radiated spectrum of GCs. Cumulative pulsed curvature radiation (CR) from an ensemble of millisecond pulsars (MSPs) embedded in a GC leads to a detectable GeV spectral component [10–12]. Within leptonic models, unpulsed emission may result from relativistic leptons injected by MSPs and radiating synchrotron radiation (SR) and inverse Compton (IC) emission as these particles traverse the GC [12–17]. Recent application of such a model [18] resulted in a reasonable fit to the broad spectral energy density (SED) of Terzan 5: the hybrid model invokes unpulsed SR and IC components to model the radio and TeV data as well as cumulative pulsed CR to fit the *Fermi* LAT data and pulsed SR from electron-positron pairs within the pulsar magnetospheres to explain the hard *Chandra* X-ray spectrum. Additionally, [19] found that tens of Galactic GCs may be detectable within a reasonable amount of observation time by the next-generation Cherenkov Telescope Array (CTA). Other models assume white dwarfs that inject relativistic leptons into the GC [20], or a gamma-ray burst remnant that accelerates hadronic particles and secondary leptons that in turn contribute to the high-energy emission from GCs [21]. Conversely, a combination of cumulative CR emission from MSPs and dark matter annihilation could perhaps also explain the GeV emission detected by *Fermi* LAT from 47 Tucanae [22].

A general conclusion from the modelling seems to be that they predict quite a wide range of fluxes, depending on the number of free model parameters, and how well constrained they are. This proceedings article provides a summary of our assessment of uncertainties in the predicted VHE flux of GCs for a given leptonic model, strictly due to parameter uncertainties [23]. We find that one cannot simply scale the model output among different GCs, since the range of predicted fluxes depends crucially (sometimes non-linearly) on the unique input parameters plus their uncertainties per source. We advocate using a population approach and stacked upper limits to further reduce uncertainties in model predictions. We will investigate three cases in particular: a population of GCs for which *integral* flux upper limits were derived by H.E.S.S., and a Northern-hemisphere cluster, M15, and a Southern-hemisphere one, ω Cen, for which *differential* flux upper limits exist. We find that there are indeed regions in parameter space for which the stringent stacking upper limits are satisfied, given parameter uncertainties.

In Section 2, we briefly discuss the model and its free parameters. In Section 3, we discuss the method employed to calculate the IC flux expected from the GCs plus its errors derived using a Monte Carlo process. Section 4 describes the results while in Section 5 we offer our conclusion.

2. Model

Here, we focus on the VHE component. We use the model by [17] to calculate the particle transport (diffusion and radiation losses) in a spherically symmetric, stationary approach. We then predict the TeV spectral component for GCs due to the cumulative IC by leptons injected by a population of MSPs into the GC. The seven main free parameters of this model are [18, 19]: cluster magnetic field (B), power-law index (Γ) of the injected particle spectrum, number of GC stars (N_*), distance to the cluster (d), the average spin-down luminosity per pulsar ($\langle \dot{E} \rangle$), the conversion efficiency of spin-down luminosity into particle acceleration (η), and number of MSPs in the GC ($N_{\rm MSP}$). We fixed the minimum and maximum particle energies, spatial diffusion coefficient (κ), the core radius ($r_{\rm c}$), the half-mass radius ($r_{\rm h}$), and the tidal radius ($r_{\rm t}$) for each GC. After solving for the particle spectrum in different spatial zones, we predict the emission properties of each zone, and finally obtain the spatially-dependent differential and integral VHE flux via a line-of-sight calculation.

3. Monte Carlo method

Our first case study entails the prediction of the cumulative TeV flux from the 15 Galactic GCs observed by H.E.S.S., and comparing this with their *integral* flux upper limits. We use the method of [14] and calculate the single-GC and stacked integral VHE flux of 15 GCs [6], with uncertainties due to the uncertainty in model parameters. We randomise over the seven free parameters(B, Γ, N_*, d, η, $\dot{E}$ and $N_{\rm MSP}$), but fix the structural and diffusion coefficient parameters. First, we set the source strength $Q_0 = 1$ and only use four free parameters (B, Γ, N_*, and d). We calculate the integral flux and obtain a spread of fluxes, finding that a finer parameter sampling grid lead to a smoother distribution of fluxes. Second, we find convergence of the flux distribution with an increase of the number of trials. We thus note that undersampling does not give a smooth flux distribution, but oversampling indeed leads to convergence. Lastly, we perform nested loops over all seven free model parameters to calculate $Q_0(\Gamma, \eta, \langle \dot{E} \rangle, N_{\rm MSP}) \neq 1$, and multiply the correct flux, pre-calculated for $Q_0 = 1$ and depending only on B, Γ, d, and N_*, by the actual value of Q_0. The spread in flux reflects the uncertainty in model parameters, and as the number of trials is increased, a smoother distribution of predicted flux results.

Our second and third case studies involve *differential* flux predictions for M15 and ω Cen. We again use the method of [14] to estimate the uncertainty in the differential flux of M15 at 13 different observer-defined energy bins [8]. See [23] for details on the chosen parameter grids and number of trials.

4. Results

We study two parameter combinations (ranges) when attempting to satisfy the H.E.S.S. upper limits. In this way, we note how the stringent stacking upper limit points to a constraint on initial best-guess parameter ranges.

The first set (range) of parameter combinations is as follows: $d' \in \left[\frac{d}{2}, \frac{d}{\sqrt{2}}, d, \sqrt{2}d, 2d\right]$, $N'_* \in \left[\frac{N}{2}, \frac{N_*}{\sqrt{2}}, N_*, \sqrt{2}N_*, 2N_*\right]$ (see [23] for values of d and N_*), $B \in [1, 9]$ in steps of 2μG,

Table 1: H.E.S.S. flux upper limits [6] and model predictions for the first set of parameter combinations. The columns are: the GC name; analysis energy threshold (TeV); integral photon flux upper limits $F_{\rm UL}(E > E_{\rm th})$ in units of 10^{-13}photons cm^{-2}s^{-1}; median of $\log_{10}$ of integral flux distribution F_μ in same units; ratio between the σ_{16} and the median (%); ratio between σ_{84} and the median (%); ratio between the median and the flux upper limit; geometric mean in units of 10^{-13}ph cm^{-2}s^{-1}; ratio between standard deviation σ and the median (%); and the ratio between the geometric mean and median. The bottom row represents results for a stacking scenario [6].

GC name	$E_{\rm th}$	$F_{\rm UL}$	F_μ	σ_{16}/F_μ	σ_{84}/F_μ	$F_\mu/F_{\rm UL}$	$\bar{F}_G$	σ/F_μ	$\bar{F}_G/F_\mu$
NGC 104	0.72	19	0.154	86	614	0.0081	0.145	929	0.94
NGC 6388	0.28	15	0.187	82	410	0.0125	0.179	610	0.96
NGC 7078	0.40	7.2	0.053	84	573	0.0074	0.051	737	0.95
Terzan 6	0.28	21	0.218	84	463	0.0104	0.208	766	0.92
Terzan 10	0.23	29	0.356	84	475	0.0123	0.337	778	0.95
NGC 6715	0.19	9.3	0.037	82	429	0.0040	0.035	622	0.96
NGC 362	0.59	24	0.047	85	513	0.0020	0.044	923	0.94
Pal 6	0.23	12	0.343	85	578	0.0286	0.324	787	0.94
NGC 6256	0.23	32	0.101	84	482	0.0032	0.096	810	0.95
Djorg 2	0.28	8.4	0.317	84	451	0.0377	0.302	713	0.95
NGC 6749	0.19	14	0.218	84	577	0.0156	0.205	780	0.94
NGC 6144	0.23	14	0.138	86	492	0.0097	0.129	819	0.93
NGC 288	0.16	5.3	0.196	85	492	0.0370	0.183	806	0.93
HP 1	0.23	15	0.172	85	481	0.0115	0.162	797	0.95
Terzan 9	0.33	45	0.090	87	580	0.0020	0.084	1147	0.93
Stacking	0.23	3.3	0.895	48	108	0.271	0.923	113	1.03

$\Gamma \in [1.7, 2.9]$ in steps of 0.3, $\eta \in [0.005, 0.08]$ in steps of 0.0075, $\log_{10}\langle\dot{E}\rangle \in [33.7, 34.7]$ in steps of 0.1, and $N_{\rm MSP} \in [5, 150]$ in steps of 10. Since our flux distributions appear to be approximately log-normal, we first obtain the median flux F_μ (50$^{\rm th}$ percentile) as well as the 16$^{\rm th}$ and 84$^{\rm th}$ percentile for the single GCs. We also calculate $\sigma_{16} = \mu - F_{16}$ and $\sigma_{84} = F_{84} - \mu$, and study them as percentages: $100\sigma_{16}/\mu$ and $100\sigma_{84}/\mu$, with F_{16} and F_{84} being the 16$^{\rm th}$ and 84$^{\rm th}$ percentiles. We obtain the geometric mean of the flux $\bar{F}_{\rm G}$ as well as the standard deviation σ of this flux. We finally calculate the ratios $F_\mu/F_{\rm UL}$ as well as $\bar{F}_{\rm G}/F_\mu$, indicating that $F_\mu \approx \bar{F}_{\rm G}$. For the weighted (stacked) flux, we set the threshold energy to $E_{\rm th} = 0.23$ TeV and calculate $F_{\rm w} = \sum_{i=1}^{15} \frac{\tau_{\rm i}}{\tau_{\rm tot}} \times F_i(> 0.23$ TeV), where i represents a specific GC, τ_i is the live time for each GC, and $\tau_{\rm tot}$ is the total live time.

We found that for this initial choice, the median stacked flux exceeds the upper limit by a factor of 7.6. We therefore considered a second parameter set (Table 1): $\eta \in [0.003, 0.03]$ in steps of 0.003, $\log_{10}\langle\dot{E}\rangle \in [33, 34]$ in steps of 0.1, and $N_{\rm MSP} \in [5, 50]$ in steps of 5. There is no unique way of reducing the GC flux. Thus, we reduced the three (degenerate) main parameters determining the source strength Q_0, i.e., η, $\dot{E}$, and $N_{\rm MSP}$ by a factor of a ~ 3 each to illustrate that by lowering Q_0, the flux upper limits may be satisfied. In this case, the predicted median flux is a factor of ~ 4 below the H.E.S.S. upper limit.

We summarise the fluxes we obtained for both the stacked as well as single-GC cases in Figure 1.

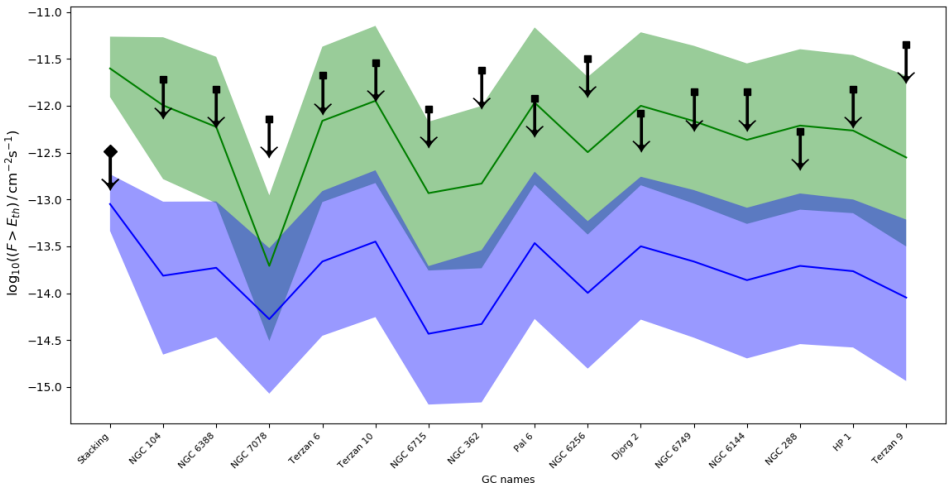

Figure 1: Flux upper limits (black diamond and squares with arrows) on the observed gamma-ray flux from the population of GCs, as well as the predicted flux medians plus 1σ uncertainties (green and blue) for each of the two parameter combinations. The first entry indicates the stacked flux with 1σ uncertainties.

The black diamond and squares and arrows correspond to the observational upper limits, while the green and blue squares and error bars are for the median fluxes and 1σ uncertainty intervals, for the two different parameter combinations as discussed above. Thus, there are indeed parameter combinations that yield fluxes below all of these observational upper limits.

Our second case study involves M15, which was recently observed at low zenith angles by MAGIC [8]. They found an upper limit of $F(E > 0.3\ \mathrm{TeV}) = 3.2 \times 10^{-13}\ \mathrm{cm}^{-2}\mathrm{s}^{-1}$, which several times more stringent than the $F(E > 0.44\ \mathrm{TeV}) = 7.2 \times 10^{-13}\ \mathrm{cm}^{-2}\mathrm{s}^{-1}$ published earlier by [6]. We create a distribution of differential fluxes for energy bins 2 and 7 (centred on energies of $E = 62$ GeV and $E = 955$ GeV) and calculate the median and 1σ uncertainties of the $\log_{10}$ of these fluxes by finding the 16^{th}, 50^{th} and 84^{th} percentiles. Figure 2 shows the upper limits from 165 hrs of MAGIC observations on the differential flux, the predicted spectrum for a few different combinations of model parameters, and the median points with 1σ error. For our choice of parameters, we satisfy the MAGIC flux upper limits.

Our third case study involves ω Centauri (NGC 5139). It is the most massive, complex, brightest, and has the largest core and half-light radius of all GCs in the Galaxy [1], and is furthermore suspected to harbour a black hole with total mass $\sim 10^5 M_\odot$ at its centre. The Parkes Radio Telescope has now detected five radio MSPs in this cluster, but no pulsations in the GeV data have been found [24]. In Figure 3 we compare our predicted differential fluxes with the H.E.S.S. and CTA sensitivity curves for 100 hours of observations. We also indicate typical predicted gamma-ray spectra for a few choices of parameter combinations.

5. Conclusions

We assessed uncertainties in the predicted VHE flux of GCs within the context of the leptonic GC model of [17], demonstrating that uncertainty in model parameters leads to a large spread in the

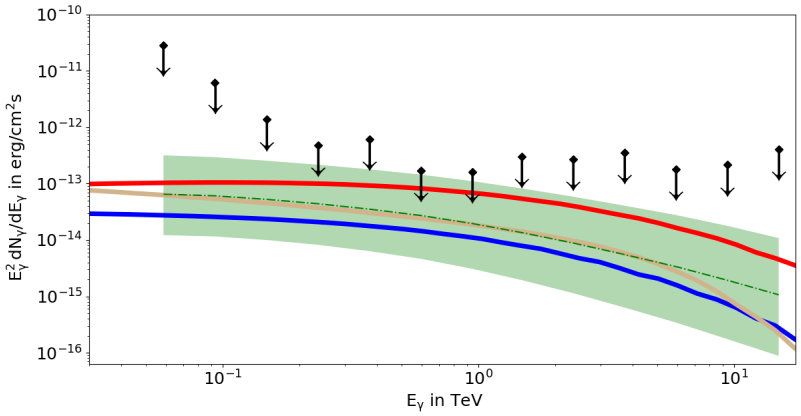

Figure 2: Differential flux upper limits (black diamonds with arrows) on the gamma-ray flux from M15 plus a few model spectra (solid lines) for typical parameter combinations, as well as predicted medians and 1σ error bars (green error band) [23].

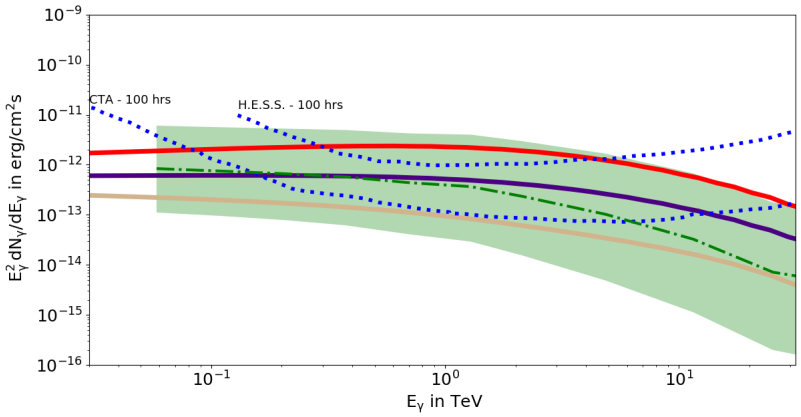

Figure 3: Differential flux predictions (green error band) for ω Cen, the solid lines indicating example predictions [23].

predicted flux. As expected, we confirmed that a finer grid in parameter space leads to a smoother flux distribution, and a larger number of trials leads to convergence of the flux distribution. Also, the eventual predicted flux range depends on the number of free parameters and their respective ranges.

While none of our predicted individual cluster median fluxes plus uncertainties violated the respective upper limits (Figure 1), our weighted flux violated the H.E.S.S. upper limit for our first set of parameter combinations, although our second parameter combination satisfied the stacked upper limits. Thus we could use this stringent upper limit to non-uniquely constrain the source properties of the MSPs embedded within the GC. For M15, we could satisfy these upper limits for typical parameters. We calculated the TeV flux for ω Cen, indicating that this source may be a possible candidate to be observed by H.E.S.S. or CTA.

Increasing measurement accuracy on model parameters will improve predictions of GC fluxes,

and this will provide better guidance to CTA's observations. Future models will have to undergo continued scrutiny, taking into account the effect of parameter uncertainty on their predictions as they are confronted with new data.

Acknowledgments

We also acknowledge discussions with James Allison and Leonard Santana. This work is based on the research supported wholly / in part by the National Research Foundation of South Africa (NRF; Grant Numbers 87613, 90822, 92860, 93278, and 99072). The Grantholder acknowledges that opinions, findings and conclusions or recommendations expressed in any publication generated by the NRF supported research is that of the author(s), and that the NRF accepts no liability whatsoever in this regard. The Virtual Institute for Scientific Computing and Artificial Intelligence (VI-SCAI) is gratefully acknowledged for operating the High Performance Computing (HPC) cluster at the University of Namibia (UNAM). VI-SCAI is partly funded through a UNAM internal research grant. This study was financially supported by the African German Network of Excellence in Science (AGNES), through the "Programme Advocating Women in Science, Technology, Engineering and Mathematics".

References

[1] W.E. Harris, *A Catalog of Parameters for Globular Clusters in the Milky Way*, *AJ* **112** (1996) 1487.

[2] A.A. Abdo et al., *A Population of Gamma-Ray Millisecond Pulsars Seen with the Fermi Large Area Telescope*, *Science* **325** (2009) 848.

[3] P.H.T. Tam, A.K.H. Kong, C.Y. Hui, K.S. Cheng, C. Li and T.-N. Lu, *Gamma-ray Emission from the Globular Clusters Liller 1, M80, NGC 6139, NGC 6541, NGC 6624, and NGC 6752*, *ApJ* **729** (2011) 90.

[4] P.F. Zhang, Y.L. Xin, L. Fu, J.N. Zhou, J.Z. Yan, Q.Z. Liu et al., *Detection of gamma-ray emission from globular clusters M 15, NGC 6397, NGC 5904, NGC 6218 and NGC 6139 with Fermi-LAT*, *MNRAS* (2016) .

[5] A. Abramowski et al., *Very-high-energy gamma-ray emission from the direction of the Galactic globular cluster Terzan 5*, *A&A* **531** (2011) L18.

[6] A. Abramowski et al., *Search for very-high-energy γ-ray emission from Galactic globular clusters with H.E.S.S.*, *A&A* **551** (2013) A26.

[7] M. McCutcheon, *VERITAS Observations of Globular Clusters*, *Proc. 31st ICRC, 1316, http://icrc2009.uni.lodz.pl/proc/pdf/icrc1316.pdf* (2009) .

[8] V.A. Acciari et al., *Deep observations of the globular cluster M15 with the MAGIC telescopes*, *MNRAS* **484** (2019) 2876.

[9] F. Aharonian et al., *HESS upper limit on the very high energy γ-ray emission from the globular cluster 47 Tucanae*, *A&A* **499** (2009) 273.

[10] A.K. Harding, V.V. Usov and A.G. Muslimov, *High-Energy Emission from Millisecond Pulsars*, *ApJ* **622** (2005) 531.

[11] C. Venter and O.C. de Jager, *Empirical Constraints on the General Relativistic Electric Field Associated with PSR J0437-4715*, *ApJ* **619** (2005) L167.

[12] A. Zajczyk, W. Bednarek and B. Rudak, *Numerical modelling of γ-ray emission produced by electrons originating from the magnetospheres of millisecond pulsars in globular clusters*, *MNRAS* **432** (2013) 3462.

[13] W. Bednarek and J. Sitarek, *High-energy γ-rays from globular clusters*, *MNRAS* **377** (2007) 920.

[14] C. Venter and O.C. de Jager, *Constraining A General-Relativistic Frame-Dragging Model for Pulsed Radiation from a Population of Millisecond Pulsars in 47 Tucanae using GLAST LAT*, *ApJ* **680** (2008) L125.

[15] C. Venter, O.C. de Jager and A.-C. Clapson, *Predictions of Gamma-Ray Emission from Globular Cluster Millisecond Pulsars Above 100 MeV*, *ApJ* **696** (2009) L52.

[16] K.S. Cheng, D.O. Chernyshov, V.A. Dogiel, C.Y. Hui and A.K.H. Kong, *The Origin of Gamma Rays from Globular Clusters*, *ApJ* **723** (2010) 1219.

[17] A. Kopp, C. Venter, I. Büsching and O.C. de Jager, *Multi-wavelength Modeling of Globular Clusters – The Millisecond Pulsar Scenario*, *ApJ* **779** (2013) 126.

[18] H. Ndiyavala, C. Venter, T.J. Johnson, A.K. Harding, D.A. Smith, P. Eger et al., *Probing the pulsar population of terzan 5 via spectral modeling*, *ApJ* **880** (2019) 53.

[19] H. Ndiyavala, P.P. Krüger and C. Venter, *Identifying the brightest Galactic globular clusters for future observations by H.E.S.S. and CTA*, *MNRAS* **473** (2018) 897.

[20] W. Bednarek, *Gamma-rays from electrons accelerated by rotating magnetized white dwarfs in globular clusters*, *J. of Phys* **39** (2012) 065001.

[21] W.F. Domainko, *Finding short GRB remnants in globular clusters: the VHE gamma-ray source in Terzan 5*, *A&A* **533** (2011) L5 [1106.4397].

[22] A.M. Brown, T. Lacroix, S. Lloyd, C. Bahm and P. Chadwick, *Understanding the γ -ray emission from the globular cluster 47 Tuc: Evidence for dark matter?*, *Phys. Rev. D.* **98** (2018) 041301.

[23] H. Ndiyavala-Davids, C. Venter, A. Kopp and M. Backes, *Assessing uncertainties in the predicted very high energy flux of globular clusters in the Cherenkov Telescope Array era*, *MNRAS* **500** (2021) 4827.

[24] S. Dai, S. Johnston, M. Kerr, F.o. Camilo, A. Cameron, L. Toomey et al., *Discovery of Millisecond Pulsars in the Globular Cluster Omega Centauri*, *ApJ* **888** (2020) L18.